Supporting Information

A quadratic isothermal amplification fluorescent biosensor without intermediate purification for ultrasensitive detection of cycling tumor DNA

Zhaojie Wu [1], Hongshan Zheng[1], Yongjun Bian[1], Jian Weng[1], Ru Zeng[2], Liping Sun[1*]

[1]The Higher Educational Key Laboratory for Biomedical Engineering of Fujian Province, Research Center of Biomedical Engineering of Xiamen, Department of Biomaterials, College of Materials, Xiamen University, 422 Siming Nan Road, Xiamen 361005, China

[2]Department of medical oncology, The First Affiliated Hospital of Xiamen University, Xiamen, China

Email: sunliping@xmu.edu.cn

1. Materials

Table S1. DNA sequences in this study

NOTE	Sequence (5′ to 3′)
ctDNA	TCGCTATCAAGACATCTCCGAAAGCC
Template	GGCTTTCGGAGATGTCTTGATAGCGACCTCAGCTAGATAGGTTAAACGTACTAAGT
cDNA	ACTTAGTACGTTTAACCTATCTAGC
H1	SH-TTTTTTTTTTTTGCTAGATAGGTTAAACGTACTAAGTAACCTACACACTTAGTACGTTTAA
H2	FAM-TTAAACGTACTAAGTGTGTAGGTTACTTAGTACGTTTAACCTACACACTTAG
H3	GGCTTTCGGAGA/iBHQ2dT/GTCTTGATAGCGATTCTTGTATGCTCGCTATCAAGACATCT - FAM
H4	TTAAACGTAC/iBHQ2dT/AAGTGTGTAGGTTACTTAGTACGTTTAACCTACACACTTAG - FAM
Mismatch 1	TCGCTATCAAGAGATCTCCGAAAGCC
Mismatch 2	TCGGTATCAAGAGATCTCCGAAAGCC
Mismatch 3	TCGGTATCAAGAGATCTCGGAAAGCC
Random	ACAGAAGAGGAGAAGTGACAATGCAT
Wildtype	TAAGAGAAGCAACATCTCCGAAAGCC

Note: BHQ2 is Black Hole Quencher 2

2. Methods and Results

2.1 Characterization of AuNPs and H2-modified AuNPs

XRD confirms the formation of AuNPs (Figure S1a). TEM image (Figure S1b) shows that the geometrical shape of the gold nanoparticles is spherical and the size of AuNPs produced in the resveratrol medium is similar to 26 nm.

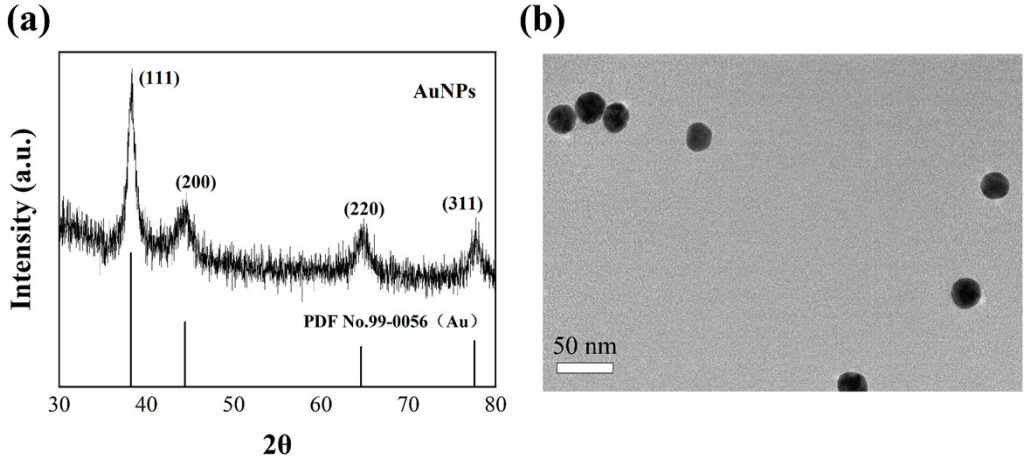

Figure S1. Characterization of AuNPs (a) XRD patterns of AuNPs (b) TEM image of AuNPs.

To verify that FAM fluorescence groups were not quenched on surface AuNPs, we compared the fluorescence intensity of the solution before and after CHA using a low concentration of H2 (50 nM). As shown in Figure S4, the fluorescence intensity of AuNPs after CHA is similar to H2 at this concentration. This indicates that AuNPs do not quench the fluorescent groups attached to their surfaces by H2. As previously reported, fluorescence groups would not be quenched at a distance of 15 nm (0.33 nm/bt, 48 bt) between fluorescence groups and the surface of AuNPs.[1]

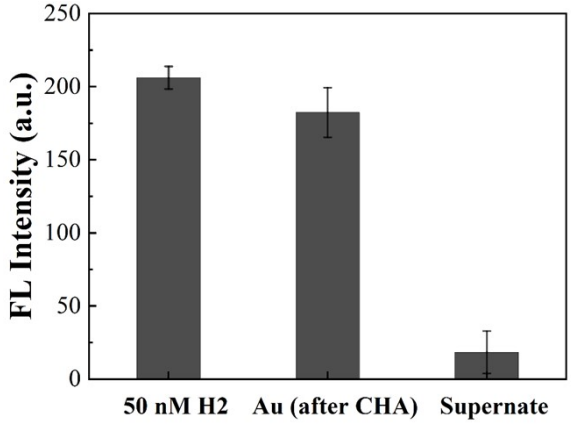

Figure S2. Comparison of fluorescence intensity in H2 and AuNPs after CHA (n = 3).

Optimization of the biosensor conditions

First, the optimum enzyme dosage, reaction temperature, and buffer liquid system can be determined according to the enzyme instruction specification from the manufacturer. Therefore, the only parameter needed to be confirmed is the optimum time of enzyme reactions. As shown in Figure S2a, the fluorescence intensity increased gradually with the extension of reaction time until reaching a platform. 2 h was selected as the best reaction time for enzyme amplification.

Then we explored the influence of H1 concentration. The experimental results (Figure S2b) demonstrated that the optimal concentration of H1 was 100 nM. The amount of H1 is too much on the surface of AuNPs, and steric hindrance will seriously impede the hybridization reaction between H1 and cDNA. We also explored the effect of H2 concentration on the results of this study. As shown in Figure S2c, the highest fluorescence intensity was obtained when the H2 concentration was 200 nM. The effects of CHA reaction time and hairpin concentration on the sensor were investigated. When the reaction time increased from 5 min to 180 min, the fluorescence intensity increased at first, reaching a plateau after 120 min (Figure S2d).

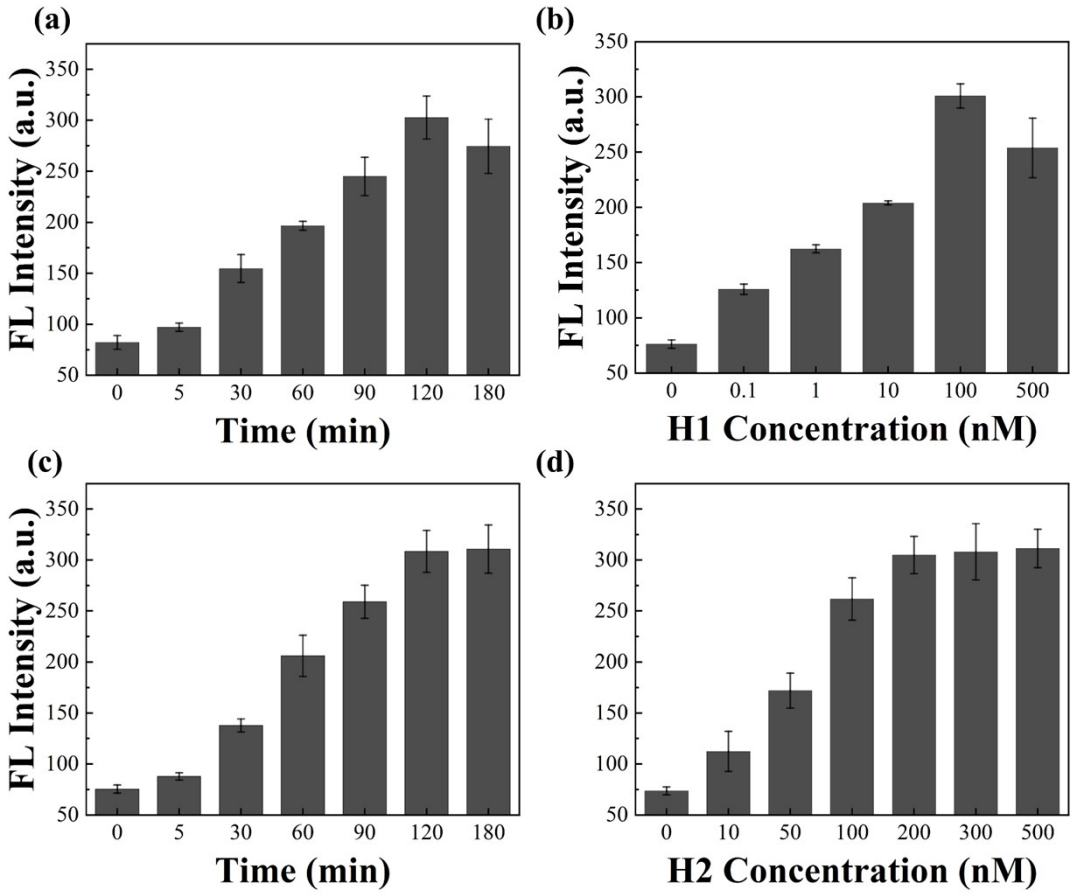

Figure S3. Optimization of reaction time and hairpin DNA concentration (n = 3). (a) Effect of the time of NEMA reaction on the fluorescence intensity. (b) Effect of the concentration of hairpin H1 on the fluorescence intensity. (c) Effect of the time of CHA reaction on the fluorescence intensity. (d) Effect of the concentration of hairpin H2 on the fluorescence intensity. All experiments were conducted at 37 °C.

2.2 Quantification of hairpin DNA modified on the AuNPs surface

The amount of H1 loaded on each AuNP is determined by measuring the fluorescence of the FAM (5-carboxyfluorescein) dye that was marked on H1. Add dithiothreitol (DTT) (final concentration is 20 mM) into the solution of the AuNP conjugated of the hairpin H1 DNA, and incubate overnight at room temperature. Then, the gold aggregates were removed by centrifugation, and the fluorescence intensity at 518 nm of the supernatant was determined by fluorescence spectrometer.

As shown in Figure S3b, the concentrations of FAM-labeled DNA were determined by interpolation fluorescence signal from a standard linear calibration curve

(Figure S3a) that was prepared with known concentrations of the oligonucleotide with identical buffer and DTT concentration. The results showed that the concentration of H1 modified on gold nanoparticles was 17.34 nM.

According to previous reports, the concentration of gold nanoparticles can be deduced as 6.56×10^{-10} mol/L from the size of AuNPs.[2] Therefore, the density of H1 = The concentration of H1 modified on gold nanoparticles /The concentration of AuNPs = 17.34 nM / 0.656 nM = 26.4 probes/particle.

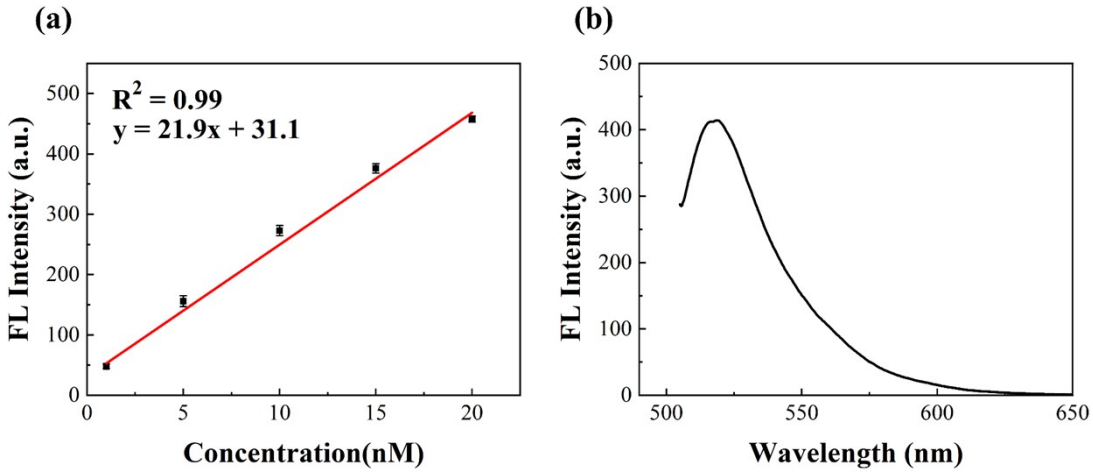

Figure S4. (a) Standard curve of H1 (n = 3). (b) Fluorescence spectra of H1 that modified on gold nanoparticles by dealing with DTT.

2.3 Calculation of the amplification efficiency

According to the manufacturer's instruction, one unit of Klenow fragment can catalyze the incorporation of 10 nmol of deoxyribonucleotides into a polynucleotide fraction in 30 min at 37°C (0.33 nmol·min^{-1}·U^{-1}), while 1 unit of NB.BbvCI can completely digest 1 μg of DNA in a 50 μl reaction in 60 minutes (0.46 pmol·min^{-1}·U^{-1}). After binding with ctDNA (26 bp), the template DNA (56 bp) necessitates amplification of an additional 30 deoxynucleotides (Figure S5). Taking 1 nM ctDNA for example, in the 50 μl reaction system, 5×10^{-5} nmol template DNA, 2.5 U Klenow fragment, and 5 U NB.BbvCI were involved in the reactions. The reaction time for NEMA was 0.023 min per round according to Formula 1. Hence, the signal amplification could reach 5.2×10^{3}-fold during 2 h reaction time.

$$T_{NEMA} = \frac{N_d}{V_1} + \frac{N_t}{V_2} = \frac{30 \times 5 \times 10^{-5}\, nmol}{2.5\, U \times 0.33\, nmol \cdot min^{-1}} + \frac{5 \times 10^{-5}\, nmol}{5\, U \times 0.46\, pmol \cdot min^{-1}} = 0.0\ min$$

$$\text{Amplification efficiency} = \frac{T_1}{T_{NEMA}} = \frac{120\ min}{0.023\ min} = 5.2\times10^3$$

(1)

Note. T_1: reaction time for each cycle of NEMA, N_d: numbers of deoxynucleotides to be replicated, N_t: the amount of double-stranded DNA, V_1: the activity of Klenow fragment, V_2: the activity of NB.BbvCI, T_1: total reaction time, T_{NEMA}: reaction time of one cycle of NEMA.

According to previous reports,[3] the reaction rate of CHA is 0.04 nmol/min. In a 50 ul reaction system with 1 nM cDNA, the reaction time for CHA is 1.25×10^{-3} min per round according to Formula 2. Consequently, the signal amplification of CHA could reach 9.6×10^3-fold during 2 h reaction time.

$$T_{CHA} = \frac{N_{cDNA}}{V_3} = \frac{5 \times 10^{-5}\, nmol}{0.04\, nmol \cdot min^{-1}} = 1.25 \times 10^{-3}\, min$$

$$\text{Amplification efficiency} = \frac{T_2}{T_{CHA}} = \frac{120\ min}{1.25 \times 10^{-3}\ min} = 9.6 \times 10^3$$

（2）

Note. T_2: the reaction time for each cycle of CHA, N_{cDNA}: the amount of cDNA, V_3: reaction rate of CHA, T: total reaction time, $T_{CHA:}$ reaction time of one cycle of CHA.

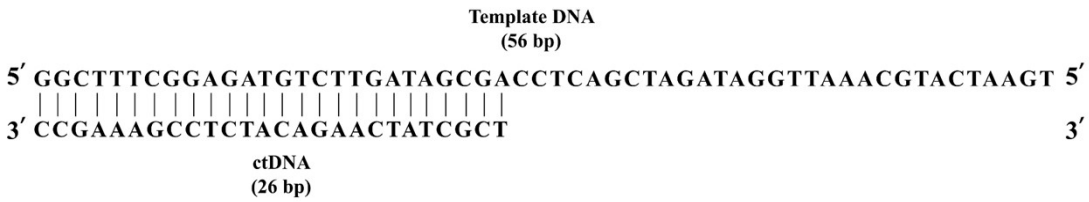

Figure S5. Schematic representation of template DNA bound to ctDNA.

Table S2. Products of NEMA and their effects on CHA

Products of NEMA	Effects on CHA
template DNA	**No**
ctDNA	**No**
cDNA	**Yes**
non-specific DNA products	**No**
NB.BbvCI	**No**
Klenow fragment	**Yes**

2.4 Structures of Klenow fragment and NB.BbvCI

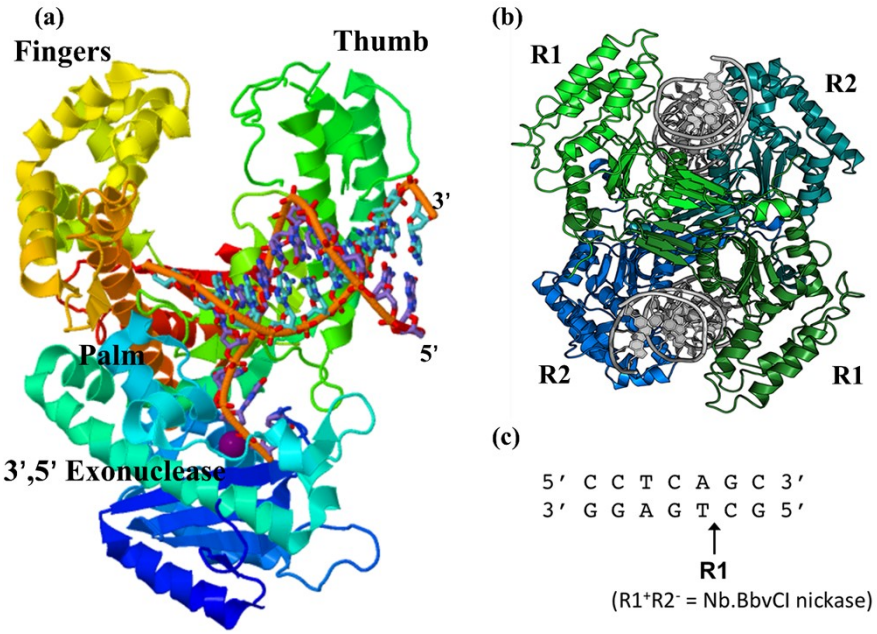

Figure S6. (a) Structure of Klenow fragment[4] (Based on an X-ray structure by Thomas Steitz, Yale

University. PDB ID: 1KLN). (b) Structure of Nb.BbvCI.[5] (c) recognition site of Nb.BbvCI and the positions of strand-cleavage catalyzed.[5]

Table S3. The amplification strategies and sensitivity of fluorescence biosensors

Amplification strategy	Target	Detection limit	Reference
CHA	DNA	19 pM	[6]
RCA and FRET	ctDNA	60 fM	[7]
NEMA	ctDNA	0.16 fM	[8]
RCA	miRNA	6.4 pM	[9]
ZrMOF	DNA	2 fM	[10]
CQDs	miRNA	4.7 fM	[11]
MB probes, and LAMP	ctDNA	20 fM	[12]
HCR and copper nanoclusters	miRNA	1.7 pM	[13]
DNAzyme and HCR	miRNA	7.9 fM	[14]
NDFPs and CHA	miRNA	1 fM	[15]
NEMA and FRET	miRNA	70.9 fM	[16]
ERA, RCA and AgNCs	DNA	1.4 fM	[17]
AuNPs and DSN	miRNA	45 fM	[18]
RCA and DNAzyme	ctDNA	43 fM	[19]
G-quadruplex and CRISPR/Cas12a	ctDNA	2 pM	[20]
NEMA and CHA	ctDNA	2 aM	This work

Abbreviations:
RCA: rolling circle amplification
FRET: fluorescence resonance energy transfer
NDFPs: nanostructure-based dual-color fluorescent probes
CHA: catalytic hairpin assembly
HCR: hybridization chain reaction
AgNCs: silver nanocluster
ERA: exoIII recycling amplification
MB: molecular beacon
LAMP: loop-mediated isothermal amplification

ZrMOF: zirconium porphyrin MOF nanoparticles
CQDs: carbon quantum dot
DSN: duplex-specific nuclease

Table S4. Physicochemical properties of proteins in human serum

Name	Content (%)	Relative molecular mass (Da)	Isoelectric point
Albumin	57-58	~69000	~ 4.7
α_1-globulin	1.0-5.7	~200000	~ 5.3
α_2 globulin	4.9-11.2	~3000000	~ 5.1
β-globulin	7.0-13	90000~150000	~ 5.2
γ-globulin	9.8-18.2	156000~3000000	~ 7.1

References

1. P. Anger, P. Bharadwaj and L. Novotny, *Physical review letters*, 2006, **96**, 113002-113002.
2. W. Haiss, N. T. K. Thanh, J. Aveyard and D. G. Fernig, *Analytical Chemistry*, 2007, **79**, 4215-4221.
3. Z. Qing, J. Hu, J. Xu, Z. Zou, Y. Lei, T. Qing and R. Yang, *Chemical Science*, 2020, **11**, 1985-1990.
4. R. K. Mohanty, S. Thennarasu and A. B. Mandal, *Colloids and Surfaces B-Biointerfaces*, 2014, **114**, 138-143.
5. B. W. Shen, L. Doyle, P. Bradley, D. F. Heiter, K. D. Lunnen, G. G. Wilson and B. L. Stoddard, *Nucleic Acids Research*, 2019, **47**, 450-467.
6. Z. Duan, Z. Li, J. Dai, H. He and D. Xiao, *Talanta*, 2017, **164**, 34-38.
7. Mariia, Dekaliuk, Xue, Qiu, Frédéric, Troalen, Pierre, Busson, Niko and Hildebrandt, *ACS sensors*, 2019, **4**, 2786-2793.
8. W. Zhou, L. Wang, C. Liu, Q. Teng, Z. Wang and Z. Dai, *Chem. Sci.*, 2020, **11**, 3745-3751.
9. X. Huo, Z. Shuxin, O. Changhe, W. Zhenmeng, W. Dong, L. Yiyun, J. Yifan and W. Zai-Sheng, *Talanta*, 2018, **192**, 175-181.
10. S. Liu, Y. Huo, L. Fan, B. Ning, T. Sun and Z. Gao, *Analytica chimica acta*, 2022, **1192,** 339340.

11. D. Wu, H. Du, X. Yan and G. Jie, *Microchemical Journal*, 2022, **183,** 108116.
12. M. Varona, D. R. Eitzmann, D. Pagariya, R. K. Anand and J. L. Anderson, *Analytical Chemistry*, 2020, **92**, 3346-3353.
13. S. Sadeghi and M. Rahaie, *Journal of Fluorescence*, 2022, **32**, 2297-2307.
14. R. Wang, L. Wang, X. Xu and W. Jiang, *Sensors and Actuators B: Chemical*, 2018, **268**, 287-292.
15. B. Li, Y. Liu, Y. Liu, T. Tian, B. Yang, X. Huang, J. Liu and B. Liu, *ACS Nano*, 2020, **14**, 8116-8125.
16. X. Chen, K. Xu, J. Li, M. Yang, X. Li, Q. Chen, C. Lu and H. Yang, *Biosensors & Bioelectronics*, 2020, **155,** 112104.
17. N. Wu, H.-C. Zhang, X.-H. Sun, F.-N. Guo, L.-X. Feng, T. Yang and J.-H. Wang, *Sensors and Actuators B-Chemical*, 2022, **352,** 131041.
18. Z. Sun, J. Li, Y. Yang, Y. Tong, H. Li, C. Wang, L. Du and Y. Jiang, *Bioconjugate Chemistry*, 2022, **33**, 1698-1706.
19. S. Liu, Y. Yang, M. Shi, H. Shi, D. Mao, X. Mao and Y. Zhang, *Acs Sensors*, 2022, **7**, 658-665.
20. X. Zhao, Y. Zhou, X. Lv, H. Zhang, X. Cui, T. Gong, H. Meng, L. Yin, G. Li and B. Yu, *Sensors and Actuators B-Chemical*, 2023, **380,** 133310.